

Measurement of Resonance Fluorescence in a Laser-Produced AlXII Plasma

C. A. Back,^(1,2) R. W. Lee,⁽¹⁾ and C. Chenais-Popovics⁽³⁾

⁽¹⁾Lawrence Livermore National Laboratory, University of California, Livermore, California 94550

⁽²⁾Department of Physics, University of Florida, Gainesville, Florida 32611

⁽³⁾Laboratoire de Physique des Milieux Ionisés, Ecole Polytechnique, 91128 Palaiseau CEDEX, France
(Received 26 May 1989)

We demonstrate radiative resonant pumping using two spatially distinct laser-produced aluminum plasmas. An embedded microdot was irradiated to prepare a plasma that was predominantly in the AlXII 1^1S_0 ground state. This plasma was then pumped by a photon flux at 7.757 Å, the wavelength of the $1^1S_0-2^1P_1$ transition. The absolute measurement of the resulting fluorescent signal was $\approx 1.5 \times 10^{11}$ photons/sr.

PACS numbers: 52.25.Nr, 52.40.Nk, 52.50.Jm

Spectroscopy is an essential tool in the study of laser-produced plasmas. Initially, the identification of ion species was used to estimate plasma temperatures. Then, the analysis of emission spectra was refined to enable detailed measurements of temperature and density.¹⁻³ More recently, absorption techniques have been developed so that the experimenter can probe the plasma as well as passively observe it.⁴ However, for plasmas that are significantly affected by radiative transfer, these techniques alone do not give enough information to fully interpret the spectra.

A promising next step for plasma spectroscopy is the study of fluorescence resulting from a radiative pump. First, photopumping has never been directly observed or studied in the x-ray regime. Its effects on x-ray spectra have not been experimentally verified. Second, if a known radiative pump is used, the pump would serve as a controlled probe that perturbs the plasma and causes it to fluoresce. The study of this fluorescence would yield detailed information about radiation transport, level populations, and the competing rate processes in the plasma. Finally, the study of photopumping is directly relevant to x-ray lasing schemes that depend on this process to create population inversions.⁵ This present study begins to explore the fundamental process of photopumping itself.

The three experiments described in this Letter are the first attempt to quantify fluorescence due to controlled radiative resonant pumping. Radiative resonance pumping is the process by which the first dipole-allowed excited state is selectively populated by a photon source tuned to the transition energy between the ground and the excited state. We used a line-coincidence scheme to observe the fluorescence of the AlXII $1^1S_0-2^1P_1$ transition due to photopumping by photons produced by the same AlXII $1^1S_0-2^1P_1$ transition from a spatially different plasma source. Thus, this photopumping experiment involved two independent plasmas. In this Letter, the plasma that will be pumped is called the front plasma. The second plasma, which was created later in time and

served as the radiative pump, will be called the pump plasma. Two preliminary experiments were performed to characterize the individual plasmas separately. The third, and final, experiment combined the two plasmas to create a photopumping system.

The experiments were performed at the JANUS facility at Lawrence Livermore National Laboratory using two independent laser beams. The pulse lengths and energies were optimized to create the necessary conditions for the front and pump plasmas. The target consisted of a 24- μm -thick polypropylene substrate (CH) with an embedded microdot of 270 μm diam on one side and a 550- μm -diam spot of aluminum on the other [see Fig. 1(a)]. The embedded microdot, a 1500-Å-thick spot of Al overcoated with 1000 Å of parylene-N, was irradiated by a 1-ns beam of 1.06- μm wavelength to create the front plasma. A relatively low irradiance of 1.0×10^{12} W/cm² was used to prepare it in the AlXII ion stage. The bare Al microdot, 3000 Å thick, was irradiated by

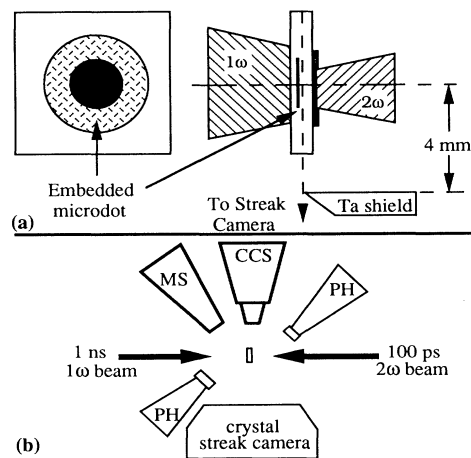


FIG. 1. (a) The target and Ta block geometry. (b) The schematic diagram of the diagnostics: pinhole camera (PH), minispectrometer (MS), curved-crystal spectrometer (CCS).

the other beam and became the pump plasma. A 0.53- μm -wavelength laser beam with a 100-ps pulse length and irradiance of 1.0×10^{14} W/cm² was used to enhance the x-ray conversion efficiency of the pump plasma. During the two-beam experiment, the peak of the laser beam that created the photon pump was delayed by 1.0 ns relative to the peak of the first laser pulse.

The front plasma was critical to the experiment because it had to be in a state that maximized the 1^1S_0 ground-state ions while minimizing the 1^1S_0 - 2^1P_1 emission. An embedded microdot was used because previous work has shown that the microdot plasma is hydrodynamically confined and has reduced temperature and density gradients.⁶ We attempted to minimize the edge effects of the irradiance by using a focal spot that was ~ 2.2 times the diameter of the microdot. The first preliminary experiment determined the conditions to create an AlXII plasma with minimum emission of the 1^1S_0 - 2^1P_1 line.

The purpose of the pump plasma was to provide a high photon flux at 7.757 Å, the wavelength of the transition to be pumped. Previous absorption spectroscopy experiments on laser-produced plasmas have used x-ray sources, called backlights, to provide a high flux of broadband radiation.⁷ The method of producing the radiative pump used in the present experiments is essentially the same as the method used to produce backlights, except that the flux must actually perturb the ions to generate a detectable fluorescence signal from the front plasma. The second preliminary experiment was performed to measure the x rays transmitted through the 24- μm -thick CH substrate. Measurements of the x-ray transmission through the CH were within 3% of the transmission predicted from the CH attenuation of the simultaneously measured pump flux. Therefore, during the photopumping experiment, the direct flux measured was used to determine the flux incident on the front plasma by correcting for the attenuation through the target.

During the final experiment, both plasmas were created. The two-sided target was supported on a special mount that had a Ta shield to physically block the pump plasma from the crystal streak camera. The camera viewed the target at 90° from the target normal. With a microscope, the knife edge of the Ta shield was aligned to within 3 μm of the middle of the CH foil when viewed edge on [see Fig. 1(a)]. The target and shield were then aligned to the vertical center line of the streak-camera photocathode slit so that the planar target was perpendicular to the plane of the photocathode. This alignment insured that the streak camera was blocked from the pump plasma but could still monitor the front plasma.

The spectroscopic diagnostics used for the final experiment [see Fig. 1(b)] covered the H-like through Li-like ion stages of Al. The preliminary experiments used a relevant subset. Time-integrating spectrometers used Bragg crystals to cover a wavelength range of 6 to 8 Å. These crystals were absolutely calibrated by measuring

the crystal rocking curve on a stationary x-ray anode source.⁸ A time-resolving streak camera was used with a Harada flat field-variable-line-spaced grating (2400 lines/mm) to measure the Li-like Al lines from the front plasma. It viewed the plasma at an angle of 45° above the axis defined by the laser beams [not shown in Fig. 1(b)] and encompassed a spectral range of 32 to 60 Å. The primary diagnostic, the crystal streak camera, overlapped the spectral coverage of the time-integrating spectrometers by using a flat potassium acid phosphate (KAP) crystal with a resolution of ~ 200 .

The preliminary front-plasma experiment showed that a laser energy of about 2 J would create a minimum emission of the 1^1S_0 - 2^1P_1 line while maintaining strong Li-like emission. Line intensities from the AlXII and AlXI stages were used for the following front-plasma line ratios: $[3^1P_1-2^1S_0]/[4^2P_{1/2}-2^2S_{1/2}]$, $[3^1P_1-2^1S_0]/[3^2P_{1/2}-2^2S_{1/2}]$, and $[4^2P_{1/2}-2^2S_{1/2}]/[3^2P_{1/2}-2^2S_{1/2}]$. These line-intensity ratios, which arise from the critical ion stages in this experiment, are a function of temperature and density, thus we are able to bracket the plasma conditions. The diagnostic ratios place the front plasmas in a range of temperatures from 200 to 400 eV with an electron density of $(5.0 \pm 0.5) \times 10^{21}$ cm⁻³.

Time-integrated line-ratio measurements in the preliminary experiment for the pump plasma determined the temperature range, density range, and the absolute photon number in the pump. We used the ratio of He-like dielectronic satellites to the AlXIII $2^2S_{1/2}$ - $3^2P_{1/2}$ line and Li-like dielectronic satellites to the AlXII 1^1S_0 - 2^1P_1 line for temperature. Density was deduced from the ratio of the same Li-like satellites to the AlXII intercombination line. These ratios give a temperature of 500–600 eV and an electron density of $(1.0 \pm 0.5) \times 10^{20}$ cm⁻³. For laser energies in the pump plasma in the range of 5.2 to 6.3 J, the absolute number of photons derived from the time-integrating spectrometer, which directly measured the pump plasma only, were on the order of 5.0×10^{12} to 1.0×10^{13} photons/sr. The transmission through the CH was measured to be $\approx 2.0 \times 10^{12}$ photons/sr.

In the photopumping experiment, the two plasmas were created with laser parameters that were determined from the first two experiments. We checked that temperatures, densities, and absolute photon numbers were comparable to those measured in the previous experiments. In addition, we checked that when only the pump plasma was created, the result on the crystal streak camera was a null spectrum. Thus, we determined that the pump radiation was effectively blocked by the Ta shield.

The crystal streak camera was used to determine the time history of the photopumping and a quantity we define as ξ , the ratio of the time-integrated recorded signal due to the self-emission to the recorded signal due to the fluorescence. Only the AlXII resonance line is observed in emission (see Fig. 2). The AlXIII lines and other AlXII are not detected even though they lie in the

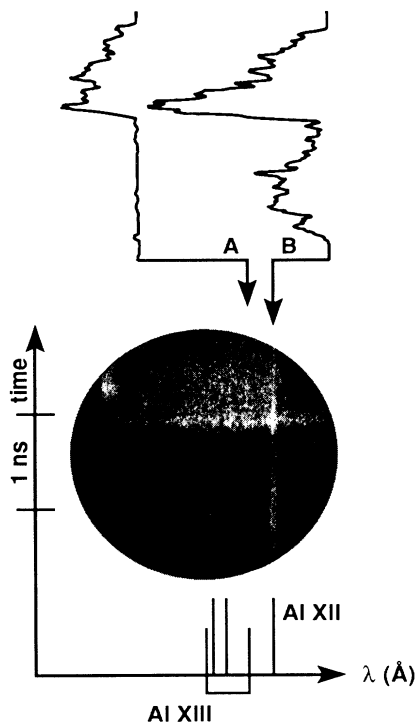


FIG. 2. Time-resolved data showing fluorescence signal. Shown in order of increasing wavelength are the positions of the strongest lines of AlXIII ($Ly-\beta$ and $Ly-\alpha$) and the other AlXII (He_γ , He_β , and He_α). The intensity plots shown above are the background emission as a function of time (A), and the AlXII $1S_0-1P_1$ emission as a function of time (B).

measured spectral range. These transitions in the front plasma are not expected to couple to the radiative pump as strongly as the resonance line because of their lower opacity. The absence of these lines, which are also the strongly emitting lines of the pump plasma during the fluorescence, indicates that the pump plasma is not directly observed.

Figure 2 shows a slice of the data centered on a line at B which corresponds to the $1^1S_0-2^1P_1$ intensity as a function of time. At low emission levels, the total signal includes background due to stray light and continuum emission. In order to correct the fluorescence data, a region near the resonance line (indicated by A in Fig. 2) was sampled to establish the base-line intensity. Figure 3 shows the AlXII $1^1S_0-2^1P_1$ emission from Fig. 2 corrected for the background. The first peak is due to the self-emission; the second peak is the fluorescence emission.

The minispectrometer recorded the initial front-plasma emission and the fluorescence. The absorption coefficient of the resonance transition is $\approx 1.77 \times 10^5 \text{ cm}^{-1}$ for the front plasma. We therefore assume that the total signal on the minispectrometer does not include the pump-plasma photons, since 99% of the pump-plasma photons will be absorbed within the first $0.2 \mu\text{m}$

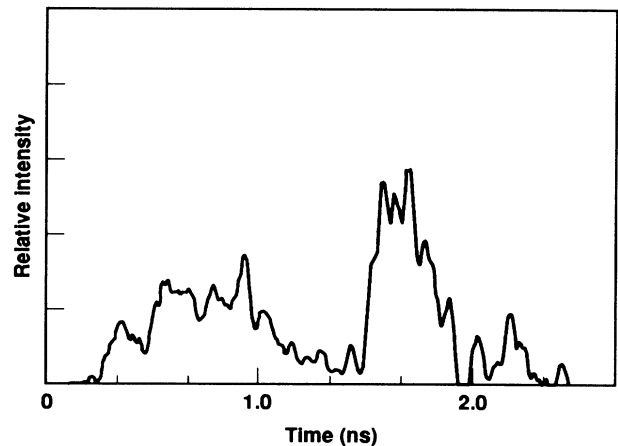


FIG. 3. Analyzed data from Fig. 2 in which the background intensity is subtracted from the AlXII $1^1S_0-1P_1$ intensity.

of the front plasma. Together, the absolute photon number and the streak-camera measurement of ξ yield a fluorescence measurement of $\approx 1.5 \times 10^{11}$ photons/sr.

An analytic estimate of the photopumping effect can be found if we use the following simple model of the plasma emission. An equivalent two-level system is used to calculate the number of ions excited to the 1^1P_1 state during each period of interest. Then, the total number of emitted photons is calculated by volume emission. Within the limits of this model we find that the ratio ξ can be reasonably approximated by the ratio of the number of photons emitted during the two periods—initial plasma formation and photopumping.

The experimental method used to produce the front plasma justifies the use of an equivalent two-level system. The primary process in the front plasma, while the laser irradiates the embedded microdot, is collisional excitation from the ground state, 1^1S_0 . However, during the radiative pumping, the stimulated-absorption rate becomes stronger than the collisional rate because the energy of the intense flux of photons is matched to the transition energy. In both cases, radiative decay is the dominant deexcitation mechanism.

Because of the combined effect of the optical depth and collisional destruction of the excited state, the detectable photons come preferentially from the plasma column edge. We will approximate the number of observable photons by the emission from the plasma region in which the optical depth, τ , is ≤ 1 . We define the active emitting volume by an annular area times a plasma length. The area has an inner radius corresponding to $\tau = 1$ for the frequency at the peak of the emergent intensity,⁹ and an outer radius corresponding to $\tau = 0$ (i.e., the radius of the microdot). For the ratio calculation, the inner radius is not a critical parameter because the area will cancel out. The length of the emitting region is different for the self-emission than for the fluorescence due to the following reasons. When the plasma is heated

TABLE I. A comparison of the calculated and experimental ratio ξ for comparable plasma conditions. $\xi(\text{calc})$ assumes an electron density of $5.0 \times 10^{21} \text{ cm}^{-3}$. The factor $V_1/V_2 \sim 20$. The third result corresponds to the data shown.

C_{0j} ($10^9/\text{sec}$)	P_{0j} ($10^{11}/\text{sec}$)	$\xi(\text{calc})$	$\xi(\text{expt})$
1.18	2.53	0.93	0.91
4.05	2.60	3.11	3.33
1.18	2.71	0.87	1.00

by the laser, the self-emission will come from the entire plasma column length, $\sim 100 \mu\text{m}$, which is determined by the ablation rate of the material. But during the photopumping, the emitting region length extends $\sim 5 \mu\text{m}$ from the absorbing region. This length, ~ 100 optical depths at the line center, is determined by the thermalization depth for the plasma conditions.⁹

The number of excitations, N_p , due to any rate, R_{0j} , from the ground state to any level j (Ref. 9) is

$$N_p = n_0 \int R_{0j} dt_p dV_p \approx n_0 R_{0j} T_p V_p,$$

where n_0 is the ion density in the ground state, T_p is the laser pulse duration, and V_p is the emitting volume. The rate is assumed to be constant over the laser pulse duration. Since we assume that every photon originating in this restricted region escapes, the ratio of the numbers excited during each phase approximately equals the ratio ξ . The initial plasma quantities are denoted by $p=1$ and the fluorescing plasma quantities are denoted by $p=2$:

$$\xi \cong \frac{N_1}{N_2} = \frac{C_{0j} T_1 V_1}{P_{0j} T_2 V_2},$$

where C_{0j} is the collisional rate (1/sec) and $P_{0j} = B_{0j} F$ (1/sec) is the photopumping rate. Here B_{0j} is the Einstein stimulated-absorption coefficient and F equals the measured flux of the pump. Table I shows the results of three shots in which the laser energy creating the front plasma varied $< 15\%$ and the photon pump was virtually the same. For an absorbing plasma near critical density, the ratio predicted by this analysis is within a factor of 2 of the ratio from the crystal-streak-camera data. The agreement of this simple model with the data indicates that the pump is efficiently coupled to the front plasma.

A detailed radiative hydrodynamic simulation now in progress will be reported later.

This paper presents the first quantitative investigation of induced fluorescence in near-critical-density laser-produced plasmas. The data prove that fluorescence due to radiative pumping can be directly and unambiguously observed. We have found the conditions for observing this effect are densities of $5.0 \times 10^{21} \text{ cm}^{-3}$ and temperatures of 200–400 eV in AlXII. For these experiments, radiative pumping was achieved for pump-plasma fluxes on the order of 2.0×10^{12} photons/sr incident on the plasma that was pumped, indicating that only modest laser energies, $\sim 6 \text{ J}$, are needed to study this technique.

The authors would like to acknowledge the helpful discussions with J. D. Kilkenny, C. F. Hooper, Jr., and J. I. Castor. We also thank the JANUS laser facility staff: J. Swain, W. Cowens, S. Mrowka, and E. Gullickson of the Lawrence Berkeley Center for X-Ray Optics. This work was performed under the auspices of the U.S. Department of Energy by Lawrence Livermore National Laboratory under Contract No. W-7405-Eng-48.

¹See review paper of C. De Michelis and M. Mattioli, Nucl. Fusion **21**, 667 (1981).

²V. A. Boiko, S. A. Pikuz, and A. Ua. Faenov, J. Quant. Spectrosc. Radiat. Transfer **19**, 11 (1976).

³J. D. Kilkenny, R. W. Lee, M. H. Key, and J. G. Lunney, Phys. Rev. A **22**, 2746 (1980).

⁴B. Yaakobi *et al.*, Rev. Sci. Instrum. **57**, 2124 (1986); J. Balmer *et al.*, Phys. Rev. A **40**, 330 (1989).

⁵P. Monier, C. Chenais-Popovics, J. P. Geindre, and J. C. Gauthier, Phys. Rev. A **38**, 2508 (1988), and references therein.

⁶M. J. Herbst, P. G. Burkhalter, R. R. Whitlock, and M. Fink, Rev. Sci. Instrum. **53**, 1418 (1982); P. G. Burkhalter *et al.*, Phys. Fluids **26**, 3650 (1983).

⁷D. L. Matthews *et al.*, J. Appl. Phys. **54**, 4260 (1983); D. W. Phillion and C. J. Hailey, Phys. Rev. A **34**, 4886 (1986).

⁸Method described in B. L. Henke and M. A. Tester, in *Advances in X-Ray Analysis*, edited by W. L. Pickles *et al.* (Plenum, New York, 1974), Vol. 18, p. 76.

⁹D. Mihalas, *Stellar Atmospheres* (Freeman, San Francisco, 1978).